

Earthquake behaviour and large-event predictability in a sheared granular stick-slip system

Fergal Dalton^{1,2} and David Corcoran¹

¹Department of Physics, University of Limerick, Ireland; email: david.corcoran@ul.ie

²Dipartimento di Fisica, Università di Roma "La Sapienza", Italy; email: fergal@idac.rm.cnr.it

March 31, 2002

Abstract

We present results from a physical experiment which demonstrates that a sheared granular medium behaves in a manner analogous to earthquake activity. The device consists of an annular plate rotating over a granular medium in a stick-slip fashion. Previous observations by us include a bounded critical state with a power law distribution of event energy consistent with the Gutenberg-Richter law, here we also reveal stair-case seismicity, clustering, foreshocks, aftershocks and seismic quiescence. Subcritical and supercritical regimes have also been observed by us depending on the system configuration. We investigate the predictability of large events. Using the quiescence between 'shock' events as an alarm condition, it is found that large events are respectively unpredictable, marginally predictable and highly predictable in the subcritical, critical and supercritical states.

Keywords: Earthquakes { model { granular { stick-slip { prediction { self-organised criticality

1 Introduction

Due to the destructive nature, and too often devastating consequences of earthquakes, it has long been the aim of seismologists to predict them. In this regard, the term "earthquake prediction" is identified with a short-term process which would specify the time, place of occurrence and size of a single earthquake with sufficient accuracy for authorities to arrange an evacuation (Main, 1997). Yet to date no undisputed earthquake prediction scheme of this type exists. Indeed, while the optimism for such a scheme was high in the 1970s (Geller, 1997), it is now questionable whether it is possible at all (Main, 1997; Geller, 1997; Evans, 1997). On the other hand, "Seismic Hazard Assessment" refers to the process by which the general likelihood of an earthquake occurring in a region is established, based on its activity history (Main, 1996). Such assessments are generally used for the coding of building practices for example and may be the best approach for reducing earthquake damage (Main, 1997).

The predictability issue of earthquakes is intertwined with the idea that earthquakes are a self-organised critical phenomenon (Bak & Tang, 1989). Short-term earthquake prediction would then be practically impossible, since the sensitivity to fluctuations at a critical point would require the details of the entire system to be known. Nevertheless, individual earthquakes have been associated with precursors, for example foreshocks, or seismic quiescence preceding an event (Main, 1996; Turcotte, 1991), and such phenomena might be used to signal the imminence of an event. Although, there is no unambiguous earthquake precursor (Main, 1997; Evans, 1997), foreshocks are recognized by the International Association of Seismology and Physics of the Earth's Interior (IASPEI) as significant possible precursors to earthquake activity, while seismic quiescence can currently be neither accepted nor rejected (Wyss, 1997).

An important difficulty in the study of earthquakes is that seismic catalogues on which earthquake statistics and analysis are based are limited both temporally and spatially. In many parts of the world, earthquake records are only decades old, while in some instances increasing and decreasing regional earthquake activity can result from the installation and removal of monitoring stations or be a consequence of isolated studies (Munoz-Diosdado & Angulo-Brown, 1999). The necessity for synthetic catalogues is clear.

Numerical models capable of generating seismicity catalogues include notably the Burridge-Knopov model and its many derivatives (Turcotte, 1997). An alternative to the numerical models, and one which is considered here, is to use a physical model. Earthquakes on a preexisting fault are assumed to be fundamentally the result of many interacting degrees of freedom subjected to a slowly increasing shear stress causing stick-slip motion. Such a definition would also have the necessary if not perhaps sufficient ingredients for a self-organized critical process. In this picture higher order features, such as quiescence, foreshocks, aftershocks and other patterns of associated earthquake activity would be expected to emerge from the system interactions. The benefit of a physical over a computational model is that it may more adequately represent or capture the entire set of physical interaction rules underlying the system. The distinction between the physical system and the well-known cellular automaton earthquake model by Olami, Feder & Christensen (OFC) (Olami et al., 1992), for example, is then primarily the rules of interaction. Generating the seismic activity from the physical experiment in this non-constrained manner, one may construct synthetic seismicity catalogues and explore these for evidence of predictability.

The paper is organized as follows. Initially, we outline a physical experiment already developed by us to study granular stick-slip motion, and explain why this might be considered as a model for earthquake activity. We highlight the previous identification by us of 3 earthquake states, critical, subcritical and supercritical and then explore the predictability of these states.

2 An Earthquake Model

The possibility that earthquake activity might be related to granular dynamics has been raised in a number of recent papers (Nasuno et al., 1997; Aharonov & Sparks, 1999; Astrom et al., 2000; Toomey & Bean, 2000). We have previously studied the stick-slip motion of a sheared granular bed (Dalton & Corcoran, 2001, 2002) using a physical experiment. The experimental apparatus consists of an annular top plate which is driven over the surface of a granular bed confined to a circular channel. The plate is driven by the action of a motor via a torsion spring. In this manner, the motor winds the torsion spring, increasing the torque on the plate. Ultimately friction can no longer sustain the applied torque, and the plate spins.

The experiment falls under the general definition for the earthquake model given above, in which the interacting degrees of freedom are the positions and velocities of individual grains determined by the forces, including friction, acting on the grains. The slowly increasing shear stress is provided by the action of the motor and torsion spring while the granular medium is in the solid phase. We consider now the dynamic behavior of the experiment to see if it is consistent with seismic activity.

We have previously found that the system behaves in a manner consistent with a self-organized critical process (Bak et al., 1987) for a subset of its operating conditions, and we have used the term "bounded self-organized criticality" to account for the finite basin of attraction of the critical state (Dalton & Corcoran, 2002). Most importantly, the distribution of event sizes in the system critical state is consistent with the Gutenberg-Richter distribution of earthquakes (Dalton & Corcoran, 2001). Events release energy E with power-law probability $p(E) \propto E^{-B-1}$, with $B = 0.88 \pm 0.04$. This lies within the range expected for real earthquakes $1.3 < B < 1.9$ (Main, 1995).

The experiment also exhibits subcritical and supercritical states of earthquake activity (Dalton & Corcoran, 2002). These states in addition to the critical state are observed in computational earthquake models (Rundle & Klein, 1993). Indeed, Lomnitz-Alder (1993) examined 40 different cases of earthquake cellular automata, and in all cases the results can be classified into one of these 3 states (Main, 1996).

Earthquake activity is also demonstrated in staircase seismicity and clustering of large events. Large events are defined here for the physical experiment as those above a threshold size where deviation from scale-invariant behavior in the power law distribution of event size occurs (see (Dalton & Corcoran, 2002) *ibid.* g. 2). Considering a representative critical experiment, g. 1 plots the cumulative number of large events (size > 10) in the system as time progresses. The 'staircase' nature of earthquake activity is clearly shown, and compares well with data of real earthquake activity in the Mexican Pacific coast (Munoz-Diosdado & Angulo-Brown, 1999). Similar results are obtained for the supercritical and subcritical states. The magnitude of all large events in the critical system is plotted as a function of time in g. 2. Activity clearly occurs in clusters,

with isolated events between. Also shown is a plot of real earthquake activity obtained from the United States Geological Survey (USGS) web-site (United States Geological Survey, 2001), for earthquakes of magnitude $M \geq 5.0$ in a circle of radius 500 km about San Francisco. Activity is clustered here also.

The activity of the apparatus, while in the representative critical state has also been considered in the temporal vicinity of a large event. To perform the analysis, the time of occurrence of all large events was extracted from the data. Activity before and after each large event was then superimposed, and the average activity about this 'stacked' or 'conglomerate' event computed. The activity considered was restricted to shock events of size $S \geq 0.1$ and was averaged over intervals of 5 s duration. The time of occurrence of the main event is denoted t_0 (in our graphs we set $t_0 = 0$). Overall, there were 104 large events, and the average shock activity was approximately $R = 0.14$ Hz (ie. one shock occurred, on average, every 7 s).

The sequence of activity following the large events is shown in fig. 3. Activity is seen to decrease from an elevated value ($R \approx 0.28$ Hz), back to the steady value in a period of 100 to 200 s. The best-fit curve to this decay is a power-law $R(t) = (t - t_0)^{-p}$, shown by the straight line $\ln R$ vs $\ln(t - t_0)$, with exponent $p \approx 0.2$. The decay is reminiscent of Omori's law where the activity of earthquakes falls off as a power-law with exponent $p \approx 1$. Variations in the power law's exponents for after shock rates have also been obtained in the computational earthquake model of Hainzl et al. (1999), where the exponent is dependent on the feedback of energy lost during an earthquake into the fault zone.

Prior to a large event, the activity decreases from the steady rate almost to zero, and then immediately before the large event, increases. Fig. 4 shows this data. Activity is largely constant at 0.14 Hz until approximately $t = -50$ s. At this point, there is a decrease to 1.9 mHz, and then an abrupt rise immediately before the main event in a power-law fashion: $R(t) = (t_0 - t)^{-q}$, $q \approx 1.6$. Thus by examining the sequence of activity about large events in the physical model, as in the case of earthquakes, aftershocks, quiescence, and foreshocks are also observed.

In the physical experiment of a sheared granular medium one therefore sees many of the characteristics of earthquake dynamics, including a power law distribution of event energy consistent with the Gutenberg-Richter law, stair-case seismicity, clustering, foreshocks, aftershocks and seismic quiescence. We conclude that the physical experiment is behaving in a manner analogous to an earthquake fault.

3 Predictability of the Earthquake Model

Given the presence of precursors, what are the implications for predictability in the representative critical state? The power-law increase in activity of fig. 4 is based on 104 large events for which 48 foreshocks were issued. However, instead of 48 of the 104 large events issuing one foreshock each, the foreshocks are due only to 25 of the large events (24%). Despite the clear change in statistical behavior as a large event is approached, the mean behavior observed describes only a small proportion of large events and thus severely limits its application for prediction purposes. It is interesting that studies of real earthquakes indicate that approximately one-quarter have foreshocks (Turcotte, 1991, 1997), in agreement with the value of 24% obtained here. Comparison of greater volumes of real and artificial data are needed to establish if this agreement holds, or is merely coincidence.

Consider now the quiescence of fig. 4 where the activity before the main shocks decreases to 1.9 mHz. This indicates that, for the 5 s interval represented by that point ($-25 \leq t - t_0 \leq -20$ s), only one of the 104 large events was active. This is clearly beyond the bounds of random probability, and hence it must be concluded that large events are almost always preceded by a quiet period 20 to 25 s before a large event. Unfortunately, the sense of this conclusion cannot be reversed. That is, it is not correct to say that a quiet 5 s interval will lead to a large event in about 20 s time. The mean rate of shocks is 0.14 Hz, so two in every seven 5 s intervals will, on average, be inactive. Hence a more detailed study of each sequence of activity is necessary.

A analysis of the data reveals that 84 of the 104 events were shortly preceded by a 40 s period in which no activity occurred and for the entire duration of the experiment, there were a total of 160 periods lasting 40 s each, in which no activity took place. Again, 84 of these led to a large event. We can use this to generate a simple prediction algorithm where a 40 s interval in which

no activity occurs is the condition upon which an "Imminent Large Event" alarm is raised. We stress that we are not proposing a novel earthquake prediction scheme here, merely presenting an analysis of our data. The 20 large events which were not preceded by an alarm can be regarded as a failure-to-predict. Furthermore, there were 76 false-alarms, also failures of the scheme, and there are a total of 84 successful predictions. Hence the success rate of this scheme is $84 / (76 + 84 + 20) = 47\%$. The false alarm rate, the fraction of alarms which are not followed by a large event, is $76 / 160 = 47\%$ and the failure-to-predict rate, the fraction of large events which are not predicted, is $20 / 104 = 19\%$.

Finally, the relationship between the duration of the quiescent period before an event to the subsequent size of the main event, is presented in fig. 5. The power-law best fit indicates an upward trend, though the data is far too poorly correlated to make any definite assumptions (correlation coefficient $r = 0.40$). Similar results are observed for earthquakes (Scholtz, 1994). The implication is that event size is effectively independent of the quiescence duration. While it might be possible to predict the imminent arrival of an event, the conclusion that must be drawn is that it is not possible to predict its size. One notes this result differs from recent computational work (Hainzlet al., 2000), in which quiescence in a modified OFC cellular automata model was shown to correlate with subsequent event size.

4 Other Earthquake States

4.1 Subcritical State

Fig. 6 is a plot of activity about 'large' events (defined here as event sizes ≥ 3) for a representative subcritical experiment. While the device still demonstrates seismic quiescence, foreshocks are not so evident and a decaying aftershock sequence is not present. Overall, in the subcritical state, it emerges that large event predictability based on quiescence is low. The optimum algorithm using a 20 s interval predicts large events with a 23% success rate, 64% false-alarms and 61% failure-to-predict.

4.2 Supercritical State

The seismicity of large events in a representative supercritical state is dominated by the recurrent large events to which this state is susceptible (Dalton & Corcoran, 2002). The events do not appear to cluster to one another. For the supercritical state, it may be true to say that the next large event ($S \geq 15$) will probably occur 200 s after the previous one. Interestingly, the torque fluctuations for supercritical data do not reveal discrete Fourier components in their power spectra (Dalton & Corcoran, 2002), though this may arise from the periodic element being lost in the dominant $1/f^2$ noise spectrum.

Activity about the large events in the supercritical state is notably different to the previous two states (see fig. 7). A precursory quiescence is still observed, though in this case, the quiescence commences at $t = 150$ s, from 0.07 Hz to zero. The zero activity is completely maintained right up to the main event excluding one shock at $t = 2.5$ s. Thus foreshocks appear to be non-existent in this state.

Aftershocks also behave in a different fashion to the critical and subcritical states. The rate of shocks is seen to decrease after the main event, following an exponential decay, to a level below the mean rate, and then, with decaying oscillations, it settles back to the mean rate. The existence of the exponential decay suggests that the apparatus is no longer operating at a critical point characterized by scale invariant power-laws. The oscillatory effect is attributed to the recurrent nature of these large events.

In the supercritical state, large events are almost perfectly predictable as the following data will demonstrate. Over the period of the experiment there were 142 large events and 144 intervals of length 100 s or longer. Each of these large events was preceded by such an interval, and so a prediction based on these parameters will have a 99% success rate, 1% false alarms and 0% failures-to-predict.

5 The General Critical State

The critical behavior marks a transition between the well defined sub and supercritical states. The latter are easily identifiable and experimentally repeatable, but the critical state has been found to exhibit a richer variety of behavior (Dalton & Corcoran, 2002). Of seven critical experiments, all exhibit qualitatively similar patterns in terms of the clustering and intermittency of large events. However, some of them have fewer large events (i.e. $S \approx 10$) and so it is necessary to reduce the threshold for 'large' events in order to make the clustering visible. The cumulative number of events obtained from four of the seven experiments tend to show a more uniform slope, attributed to this rarity of large events; rarer large events necessarily implies more frequent smaller events, leading to the more uniform slope.

The Omori-type power-law decay in aftershocks is repeated by five of the seven experiments, with exponent $0.2 \leq p \leq 0.45$. For precursory behavior, all show a quiescence beginning approximately 40 s before the main event, followed by an increase in activity in six experiments. However, the increase can only be clearly fit with a power-law in three cases, the remainder having statistics that are too low for any curve fit (with perhaps only 10 foreshocks occurring in total).

Of the seven experiments, three had similar success rate ' 47%, false alarm rate ' 48% and failure-to-predict rate ' 19%. The remaining four had success rate ' 16%, false alarm rate ' 80% and failure-to-predict rate ' 44%. This disparity may arise because the experiments with higher predictability are nearer the transition to the supercritical state where events are highly predictable. The experiments with lower predictability may similarly be near the transition to the subcritical state where large events are highly unpredictable. We note that this interpretation would also be consistent with variability in the torque value, and variability in the event size and duration distributions previously reported for the critical state (Dalton & Corcoran, 2002).

6 Conclusion

A sheared granular experiment has been shown here to behave in a manner analogous to earthquake activity and has previously been shown by us to exhibit bounded self-organised criticality. The observation of 3 distinct dynamic states, above, below and in a critical region has an important implication for the concept of self-organized criticality as applied to physical systems, specially here earthquakes. The sub and supercritical states are outside the critical region, yet in these cases and at criticality, for many different initial experimental configurations scale invariant event distributions are observed over several decades. Thus, while not perhaps self-organised critical, the experimental system is robustly self-organised to near criticality. It may be that earthquakes are similarly self-organised.

In the physical experiment, the ability of the granular material to dilate is believed to be responsible for the tuning of the system to the different system states (Dalton & Corcoran, 2001, 2002). A physical cause is therefore responsible for the observation of the different states. In actual earthquake statistics, the subjective choice of study area is known to effect the tail of the distribution, with large areas revealing sub-critical behavior and smaller areas more supercritical behavior (Main, 1996). This points to the difficulty of objectively constraining the observational data for the largest earthquakes. By studying the limits and sizes of the basins of attraction for the various states of the physical experiment, one might be able to determine the most probable tail for the scale-invariant distribution. Preliminary results (Lynch et al., 2002) suggest that the most common state for the experiment is subcritical, in agreement with recent statistical work on global earthquake data (Leonard et al., 2001).

Seismic quiescence is common to both earthquakes and large events in the experiments here. This quiescence has been utilized as a simple prediction scheme. The prediction algorithm essentially obtains the statistical likelihood of a large event occurring after a long quiescent period. From this statistical point of view, a certain level of prediction will always be possible even though the system is close to criticality, assuming a detailed history of the fault is available and the behavior is stationary.

The simple prediction algorithm implemented suggests marginal predictability for the critical state, with some experiments predictable and some not, the difference being the proximity of the specific critical state to the sub and super critical regimes. Large events in the subcritical state

seem to exhibit low predictability, while events in the supercritical state appear to be (almost) perfectly predictable.

This research has been funded by the University of Limerick Foundation and Enterprise Ireland. We are grateful to Gerry Daly for devoting considerable time and effort to this project, and acknowledge Ian Clancy and Christina Conway for useful discussions. Finally we would like to thank Ian Main for his helpful comments and suggestions while writing this paper.

References

- Aharonov E. & Sparks D., 1999. Rigidity phase transition in granular packings. *Phys. Rev. E* 60, 6890-6896.
- Astrom J.A., Herrmann H.J. & Timonen J., 2000. Granular Packings and Fault Zones. *Phys. Rev. Lett.* 84, 638-641.
- Bak P., Tang C. & Wiesenfeld K., 1987. Self-organized criticality: An explanation of the $1/f$ noise. *Phys. Rev. Lett.* 59, 381-384; Self-organized criticality. *Phys. Rev. A* 38 364-374 (1988).
- Bak P. & Tang C., 1989. Earthquake as a self-organized critical phenomenon. *Journal of Geophysical Research* 94, 15635-15637.
- Dalton F. & Corcoran D., 2001. Self-organized criticality in a sheared granular stick-slip system. *Phys. Rev. E* 63, 061312.
- Dalton F. & Corcoran D., 2002. Basin of attraction of a bounded self-organized critical state. *Phys. Rev. E* 65, 031310.
- Evans R., 1997. A assessment of schemes for earthquake prediction: editor's introduction. *Geophys. J. Int.* 131, 413-420.
- Geller R., 1997. Earthquake prediction: a critical review. *Geophys. J. Int.* 131, 425-450.
- Hainzl S., Zoller G. & Kurths J., 1999. Self-organized criticality model for earthquakes: Quiescence, foreshocks and aftershocks. *Int. J. Bifurcat. Chaos* 9, 2249-2255.
- Hainzl S., Zoller G. & Kurths J., 2000. Seismic quiescence as an indicator for large earthquakes in a system of self-organized criticality. *Geophys. Res. Lett.* 27, 597-600.
- Leonard T., Papasouliotis O. & Main I., 2001. A Poisson model for identifying characteristic size effects in frequency data: application to frequency-size distributions for global earthquakes, 'starquakes' and fault lengths. *J. Geophys. Res.* 106, 13473-13474.
- Lomnitz-Adler J., 1993. Automaton models of seismic fracture: constraints imposed by the magnitude-frequency relation. *J. Geophys. Res.* 98, 17745-17756.
- Lynch R., Corcoran D. & Dalton F., in preparation (2002).
- Main I., 1995. Earthquakes as critical phenomena: Implications for probabilistic seismic hazard analysis. *Bull. Seismol. Soc. Am.* 85, 1299-1308.
- Main I., 1996. Statistical physics, seismogenesis, and seismic hazard. *Rev. Geophys.* 34, 433-462.
- Main I., 1997. Earthquakes - long odds on prediction. *Nature* 385, 19-20.
- Munoz-Diosdado A. & Angulo-Brown F., 1999. Patterns of synthetic seismicity and recurrence times in a spring-block earthquake model. *Rev. Mex. Fis.* 45, 393-400.
- Nasuno S., Kudrolli A. & Gollub J.P., 1997. Friction in Granular Layers: Hysteresis and Precursors. *Phys. Rev. Lett.* 79, 949-952.
- Olam I.Z., Feder H.J.S. & Christensen K., 1992. Self-organized criticality in a continuous, nonconservative cellular automaton modeling earthquakes. *Phys. Rev. Lett.* 68, 1244-1247.

- Rundle J.B. & Klein W., 1993. Scaling and critical phenomena in a cellular automaton slider-block model for earthquakes. *J. Stat. Phys.* 72, 405-412.
- Scholtz C., 1994. *The Mechanics of Earthquakes and Faulting*, Cambridge University Press, Cambridge.
- Toomey A. & Bean C.J., 2000. Numerical simulation of seismic waves using a discrete particle scheme. *Geophys. J. Int.* 141, 595-604.
- Turcotte D., 1991. Earthquake Prediction. *Annu. Rev. Earth Planet. Sci.* 19, 263-281.
- Turcotte D., 1997. *Fractals and Chaos in Geology and Geophysics*, Cambridge University Press, Cambridge.
- United States Geological Survey, January 2001. "Earthquake Search: Circular Area", http://neic.usgs.gov/neis/epic/epic_circ.html.
- Wyss M. (ed), 1997. Second round of evaluations of proposed earthquake precursors. *Pure Appl. Geophys.* 149, 3-16.

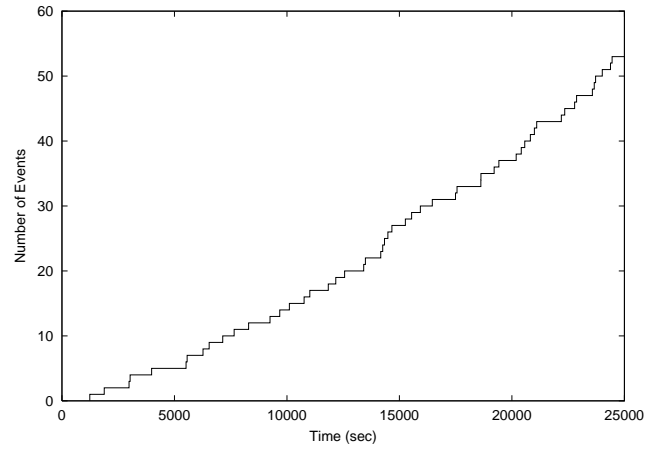


Figure 1: Cumulative number of events obtained from the apparatus for a critical state. This data is similar to plots obtained from real earthquake data.

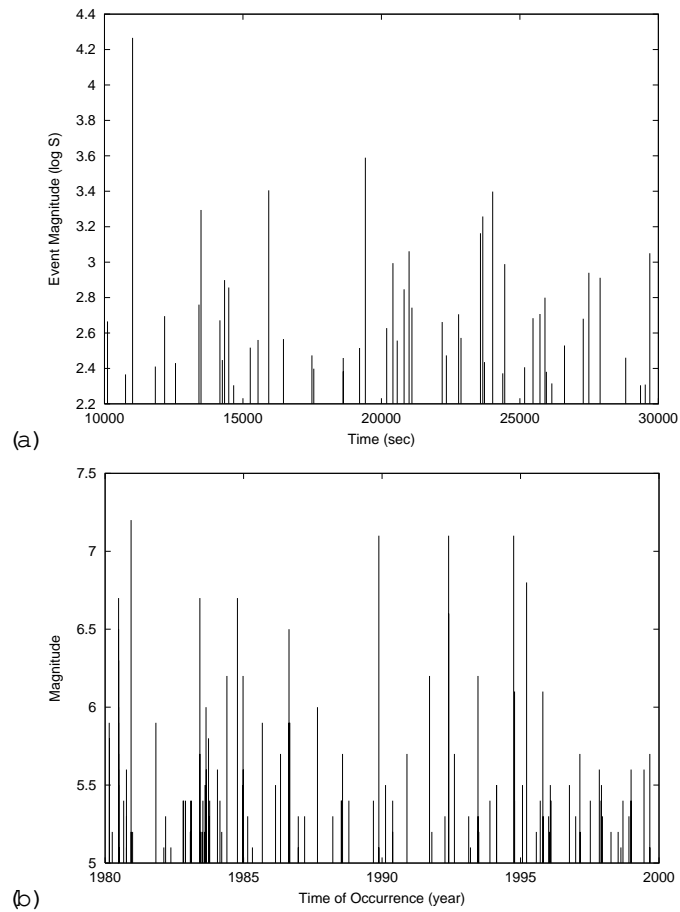


Figure 2: (a) the sequence of large events ($S \geq 10$) in the critical experiment. Note the clustering of events. (b) the sequence of large earthquakes ($M \geq 5.0$) within 500km of San Francisco in a twenty-year period. Clustering is again apparent.

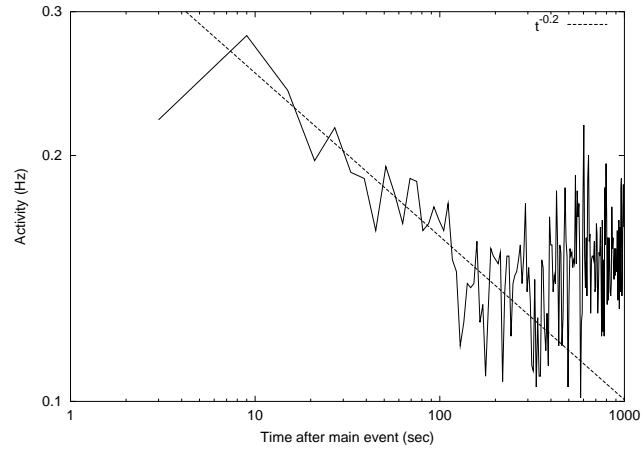


Figure 3: The aftershock activity averaged for the 104 large events of the critical experiment. There is a clear elevation in activity immediately after t_0 which decays back to the steady value $R = 0.14$ Hz.

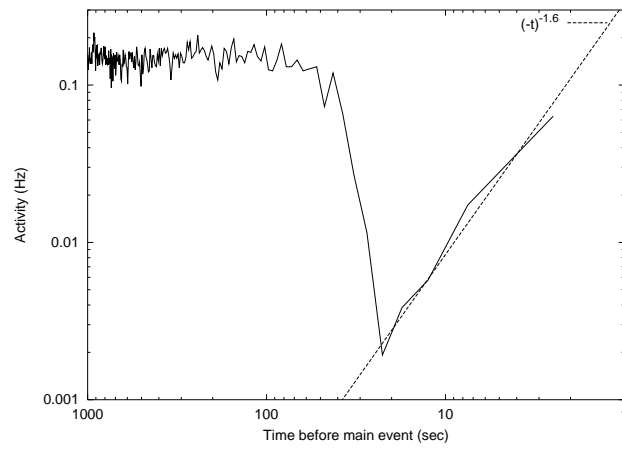


Figure 4: The averaged precursory activity before the 104 large events of the critical experiment. Activity decreases from the steady value and rapidly rises before the main event.

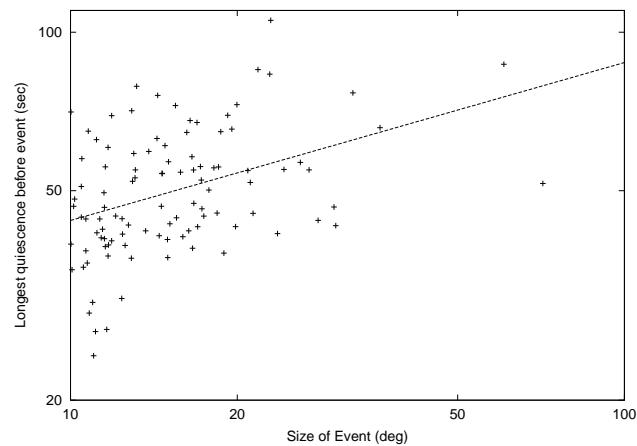


Figure 5: The longest interval preceding a large event plotted against the size of the event.

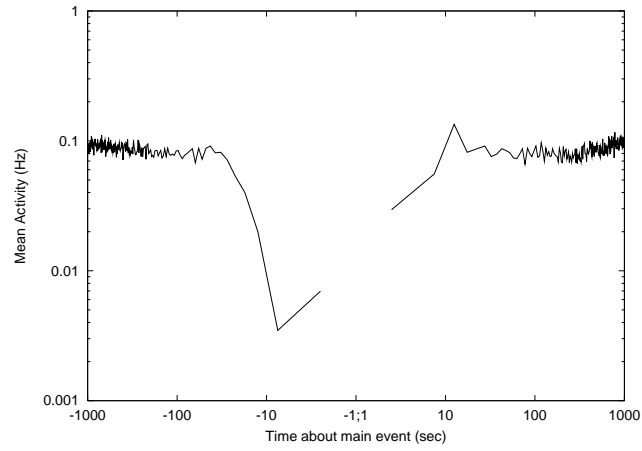


Figure 6: The activity about large events in a subcritical state. A precursory quiescence is evident, but no foreshocks or aftershocks.

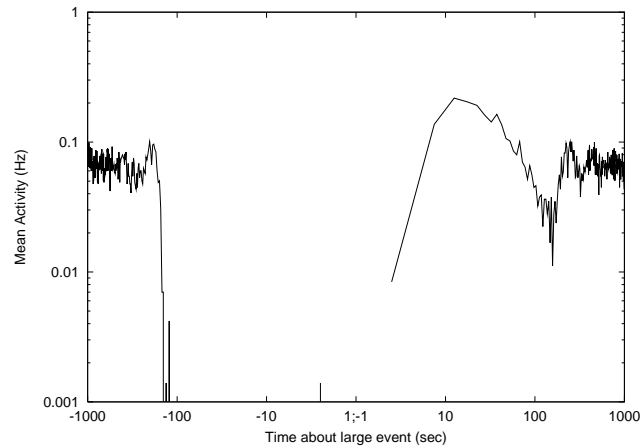


Figure 7: The averaged sequence of shocks before and after large events in the supercritical state. Activity beforehand drops from approximately 65 mHz to zero at $t = -150$ s, with only a single foreshock occurring at $t = -2.5$ s.